RSC Advances

PAPER

View Article Online
View Journal | View Issue

Cite this: *RSC Adv.*, 2018, **8**, 3782

The first colorimetric receptor for the $B_4O_7^{2-}$ anion based on nitro substituted phenanthroimidazole ferrocene derivatives†

Pei Wu, Guo Wang, Lu Zhou, Jing Lu and Jianchun Wang *

Received 23rd November 2017
Accepted 12th January 2018

DOI: 10.1039/c7ra12700f

rsc.li/rsc-advances

Four phenanthroimidazole ferrocene derivatives (**2a–2d**) were designed, synthesized and characterized by ^{1}H NMR, ^{13}C NMR and high-resolution mass spectroscopy (HRMS). Recognition of 12 anions by **2a–2d** was investigated by UV-Vis absorption analysis, showing that **2b** and **2d** sensed $B_4O_7^{2-}$ selectively among the tested anions with an obvious color change observed. ^{1}H NMR titrations and theoretical calculations demonstrated that **2b** binds $B_4O_7^{2-}$ through O···H hydrogen bonding and O···B interactions between the nitro moiety and the $B_4O_7^{2-}$ anion.

1. Introduction

Sodium borate ($Na_2B_4O_7 \cdot 10H_2O$) is an important boron-containing mineral and is used widely in the fields of glass-making, metallurgy, detergents, cosmetics, pesticides and medicines. The borate anion, or tetraborate anion, is a bicyclic structure that is composed of two BO_4 and two BO_3 moieties. A receptor for sensing the borate anion is urgently needed because about five hundred thousand tons of sodium borate is produced in China every year. The massive industrial production leads to the production of a large amount of waste water containing borate anions, and no receptor to detect this anion exists.

Imidazole is a five-membered heterocyclic aryl system that coordinates easily with metal ions to form imidazole complexes. Different structural ferrocenyl imidazole derivatives can coordinate with cations, such as Ag(I), Cu(I),[1] Pd(II), Pt(II),[2] Mo(II),[3] Mn(II), Co(II),[4] Pb(II)[5] and Hg(II),[6] to form complexes, and can be used in the recognition of cations. Imidazole can also interact with anions by hydrogen bonding, electrostatic forces and other non-covalent interactions to function as a complexing unit of an anion sensor. Ferrocene is a good sensing unit because of its excellent electrochemical properties. In 2002, Tomas and coworkers reported a simple ferrocenyl imidazolium, in which ferrocene bonded to the nitrogen of imidazole by a methylene group could interact with Cl^-, Br^-, NO_3^- and HSO_4^- anions,[7] but with broad selectivity. In recent years, a series of acyclic and trinuclear ferrocene-based imidazolium receptors noticeably improved selectivity toward the F^- anion.[8–10] Structural characterization of other ferrocenyl imidazole derivatives showed that specific recognition properties involve the ferrocene being linked directly with the C2 of imidazole, with the C4 and C5 fused to a conjugative system. One of the receptors discovered was 2-ferrocenyl-1*H*-anthra[1,2-*d*]imidazole-6,11(5*aH*,11*aH*)-dione, which was capable of detecting $[CN^-]_{aq}$ as low as ~0.1 ppm.[11] The ferrocene–imidazopyrene dyad is a simple but effective dual redox and fluorescent ion pair receptor that can detect Hg^{2+} and $H_2PO_4^-$ ions simultaneously.[12] Another ion pair sensor is the bisferrocene–benzobisimidazole triad, which acts as a multichannel receptor for selective sensing of Hg^{2+} and HSO_4^- ions.[13]

We are interested in studying the synthesis of ferrocenyl imidazole sensors[14] and the application of these sensors as cation and anion receptors.[15,16] Ferrocene moiety in these receptors raised the selectivity. It was due to the electronic properties and rigid structure of ferrocene. 2-Ferrocenyl-1*H*-phenanthro-[9,10-*d*]imidazole (**2a**) is an electrochemical switching device.[17] When studying the UV-Vis spectral response of **2a** to different ions, we found that the absorbance at 400 nm in the presence of borate and hydroxyl anions showed significant increases, but no color change to the solution was observed. In this report, a strategy was designed to introduce a nitro group to ferrocenyl imidazophenanthrene and link an acetyl group to the cyclopentadienyl (Cp) to yield novel receptors (**2b–2d**) that display better sensing responses to the borate anion.

2. Results and discussion

2.1 Synthesis of receptors

Methods for the syntheses of the receptors (**2a–2d**) are shown in Scheme 1. 2-Nitrophenanthraquinone (**d**) was prepared by the nitration of phenanthraquinone (**c**).[18] In the presence of NH_4OAc, formylferrocene and 1′-acetyl-1-formylferrocene

Department of Chemistry, Capital Normal University, Beijing 100048, P. R. China. E-mail: cnuwjc@cnu.edu.cn

† Electronic supplementary information (ESI) available. CCDC 1509214. For ESI and crystallographic data in CIF or other electronic format see DOI: 10.1039/c7ra12700f

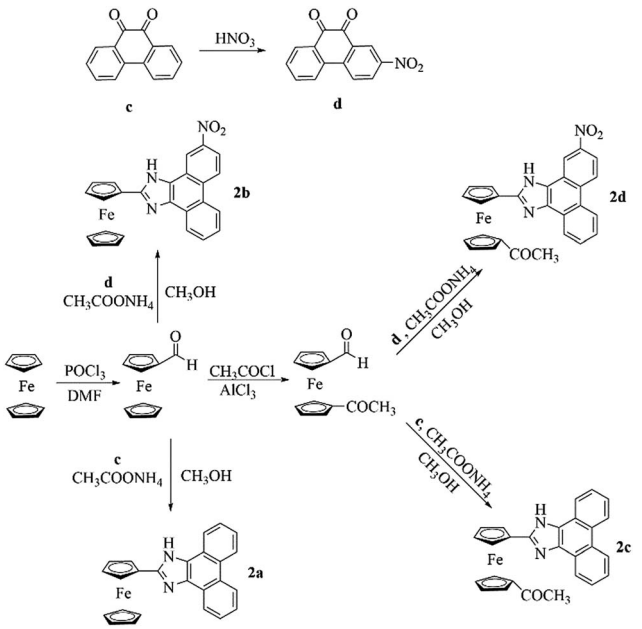

Scheme 1 Synthesis of **2a–2d**.

reacted with **c** and **d**, respectively, and underwent Radziszewski synthesis to yield the products (**2a–2d**).

2.2 X-ray diffraction single crystal structure of 2a

The X-ray diffraction single crystal structure of **2a** is shown in Fig. 1. The Fe–C bond length ranges between 2.043 and 2.059 Å. The dihedral angle of the two Cps is 0.217°, and the dihedral angle between Cp and phenanthroimidazole is 5.055°. The structure shows that Cp and phenanthroimidazole are almost parallel and form a larger conjugative system.

The rigid structure of ferrocene and phenanthroimidazole provides a specific space configuration to facilitate selectivity toward anions.

2.3 UV-Vis spectrum

The anion recognition properties of the receptors **2a–2d** toward F^-, Cl^-, Br^-, I^-, OH^-, SO_4^{2-}, SO_3^{2-}, NO_3^-, NO_2^-, $H_2PO_4^-$, AcO^- and $B_4O_7^{2-}$ were evaluated by UV-Vis spectroscopy. The solvent used in ion recognition manipulation was a mixture of DMSO and water ($V_{DMSO} : V_{H_2O} = 4 : 1$). The solutions of **2a–2d** were prepared in DMSO ($c = 1.0 \times 10^{-3}$ mol L^{-1}). All the tested anions were dissolved in water ($c = 1.0 \times 10^{-2}$ mol L^{-1}). The receptor **2a** was studied by UV-Vis spectroscopy. The absorbance at 400 nm increased dramatically when $B_4O_7^{2-}$ and OH^- were added to **2a** (Fig. 2(a)), but both anions showed the same yellow color. The receptor **2c** possesses one acetyl group more than **2a**. When the interaction of **2c** with 12 anions was investigated, we observed that the maximum absorbance in the UV-Vis spectrum of **2c** in the presence of $B_4O_7^{2-}$ was at 400 nm, whereas the absorbance maximum of the peak for **2c** in the presence of OH^- had blue shifted (Fig. 2(c)). No color change was observed. Addition of $B_4O_7^{2-}$ to **2b**, which has one more nitro group than **2a**, caused an immediate change in the color of the solution from light yellow to violet (Fig. 3). The change in the spectrum was caused by a bathochromic shift in the absorption maxima from 436 to 516 nm (Fig. 2(b)) and a change in the molar extinction coefficient from 4265 to 3890 L (mol $cm^{-1})^{-1}$, when 10 equivalents in concentration of $B_4O_7^{2-}$ was added. As shown in Fig. 5, **2b** shows higher selectivity toward $B_4O_7^{2-}$ over other anions. The receptor **2d** possesses one more acetyl group and one more nitro group than **2a**. Addition of $B_4O_7^{2-}$ to a solution of **2d** caused an immediate color change from yellow to brown (Fig. 4). Correspondingly, the absorption maxima shifted from 436 to 496 nm (Fig. 2(d)) and the molar extinction coefficient from 5628 to 6694 L (mol $cm^{-1})^{-1}$, when 10 equiv. of $B_4O_7^{2-}$ was added.

For the tested anions, receptors **2b** and **2d** possessed sensing properties only toward $B_4O_7^{2-}$. Thus, introduction of a nitro group to phenanthroimidazole resulted in a prominent color change, whereas the acetyl group showed no effect.

2.4 Competition with other anions

A competition experiment was performed to test the specificity of **2b** toward $B_4O_7^{2-}$. No significant interference was observed in the presence of competing anions and the absorbance enhancement induced by $B_4O_7^{2-}$ was retained (Fig. 6). Interestingly, all the anions were unable to decrease the absorbance of the **2b**–$B_4O_7^{2-}$ complex. Therefore, none of the anions test could alter the affinity of **2b** towards $B_4O_7^{2-}$.

2.5 UV-Vis spectral response of 2b toward a concentration gradient of $B_4O_7^{2-}$

The **2b** to $B_4O_7^{2-}$ anion complex ratio was determined. At 20 °C, titrations were carried out in a DMSO/H_2O (4 : 1) solution and the absorbance was monitored. The experiments were performed by preparing a solution (3×10^{-4} mol L^{-1}) of **2b** in DMSO/H_2O (4 : 1), followed by the addition of aqueous sodium borate (Fig. 7(a)). No obvious change in color was observed when the concentration of $B_4O_7^{2-}$ was below 1 : 2. At molar ratios of **2b** and the $B_4O_7^{2-}$ anion greater than 1 : 2, a color change to lavender was observed and the λ_{max} showed a slight red shift. The color changed to violet when the concentration of $B_4O_7^{2-}$ reached 1 equiv. to **2b**. At higher concentrations of $B_4O_7^{2-}$ no further change in the color was observed and the UV-Vis spectrum did not change either (Fig. 7(b)). This observation

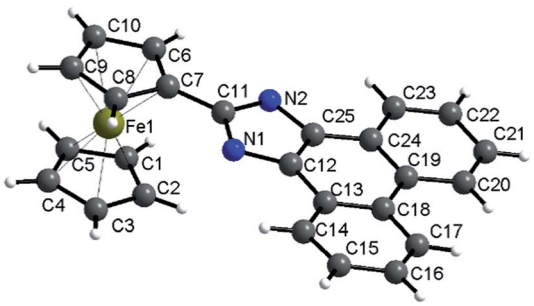

Fig. 1 Molecular structure of **2a**. CCDC: 1509214.†

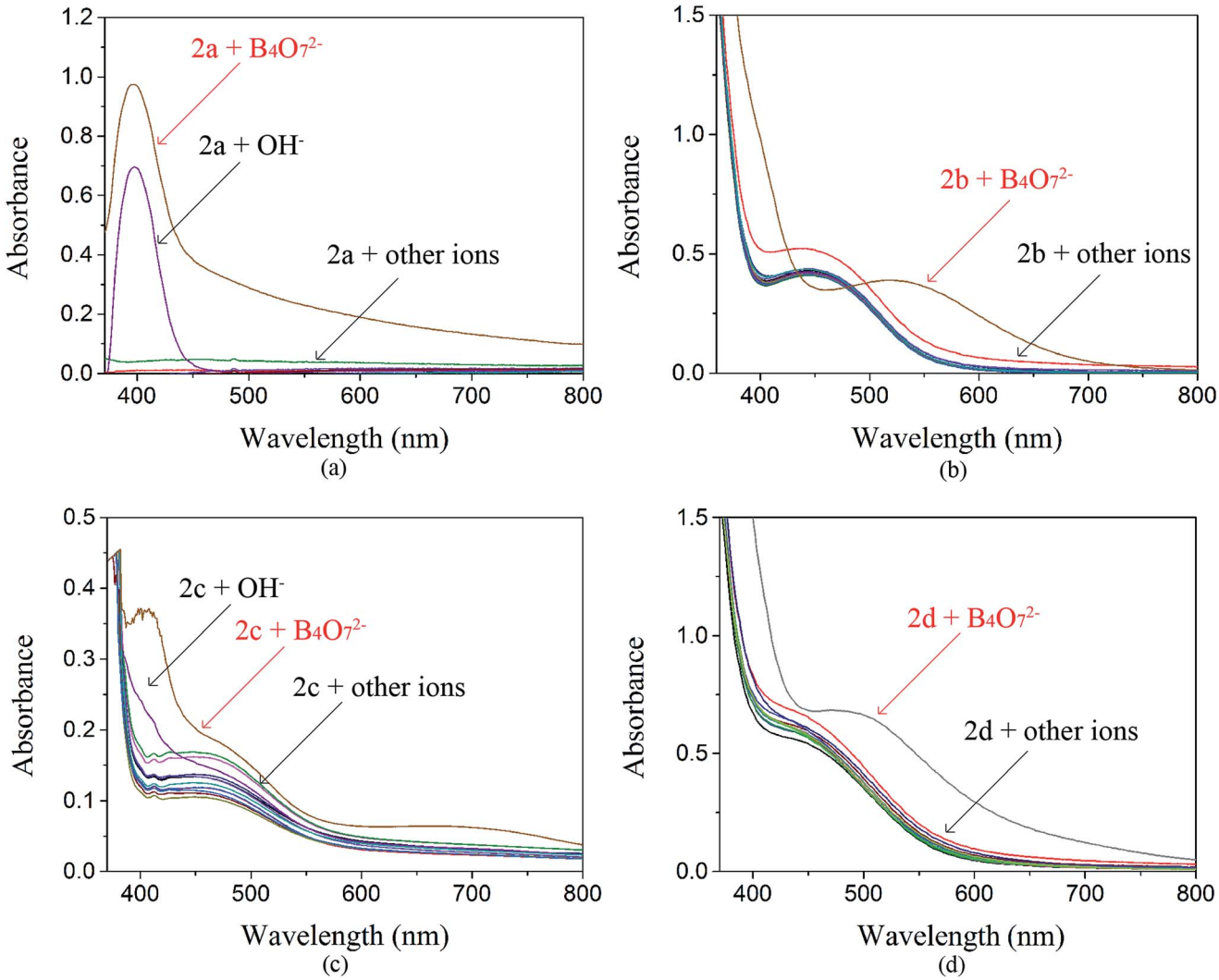

Fig. 2 Influence of various anions on the UV-Vis spectra of **2a–2d**.

Fig. 3 Influence of various anions on colorimetric properties of **2b**.

showed that the stoichiometry of the receptor **2b** to $B_4O_7^{2-}$ anion complex was 1 : 1.

2.6 Measurement of Job's plot, LOD and K_a of 2b toward the $B_4O_7^{2-}$ anion

The binding stoichiometry of **2b** with $B_4O_7^{2-}$ was examined by the Job's plot method. The presence of a maximum absorbance at a mole fraction of 0.5 shows the formation of 1 molecule of **2b** with 1 molecule of $B_4O_7^{2-}$. The binding mode is presented in Fig. 8, with a limit of detection (LOD) of 3.10×10^{-5} mol L^{-1}, as estimated by the 3σ rule (Fig. 9). The binding constant of **2b** with $B_4O_7^{2-}$ is 5.45×10^4, which was obtained from the absorbance titration data, using the Benesi–Hildebrand equation (Fig. S1†):

Fig. 4 Influence of various anions on the colorimetric properties of **2d**.

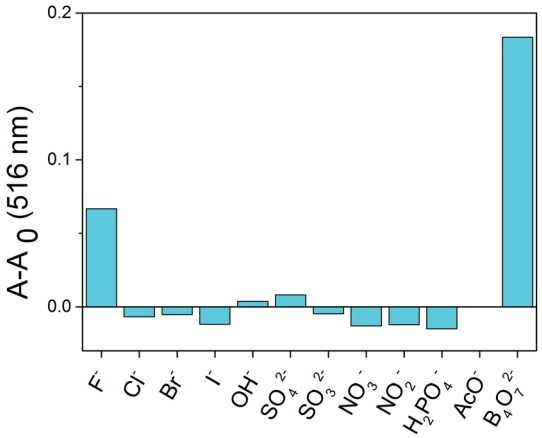

Fig. 5 Relative absorbance at 516 nm of different anions in the presence of **2b**.

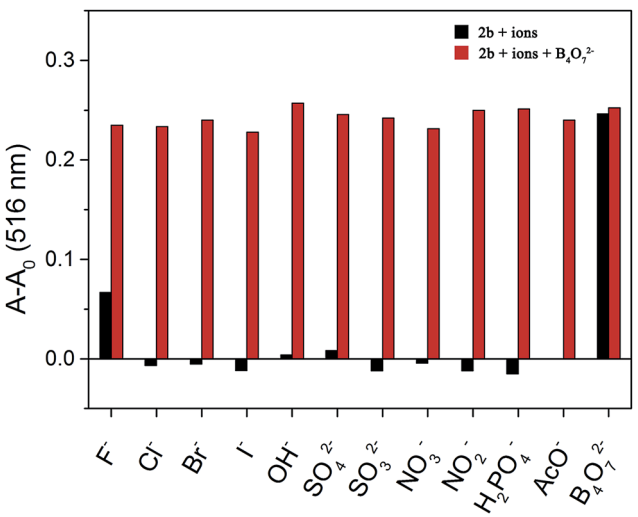

Fig. 6 Competitive selection of $B_4O_7^{2-}$ by **2b** in the presence of other anions (10 equiv. in DMSO/H_2O (4 : 1)).

$$\frac{1}{A - A_0} = \frac{1}{A' - A_0} + \frac{1}{K_a(A' - A_0)\left[B_4O_7^{2-}\right]}$$

where A_0 is the absorbance of **2b** without $B_4O_7^{2-}$, A is the absorbance with a particular concentration of $B_4O_7^{2-}$, A' is the absorbance of the fully complexed form at the highest concentration of $B_4O_7^{2-}$, and K_a is the binding constant.

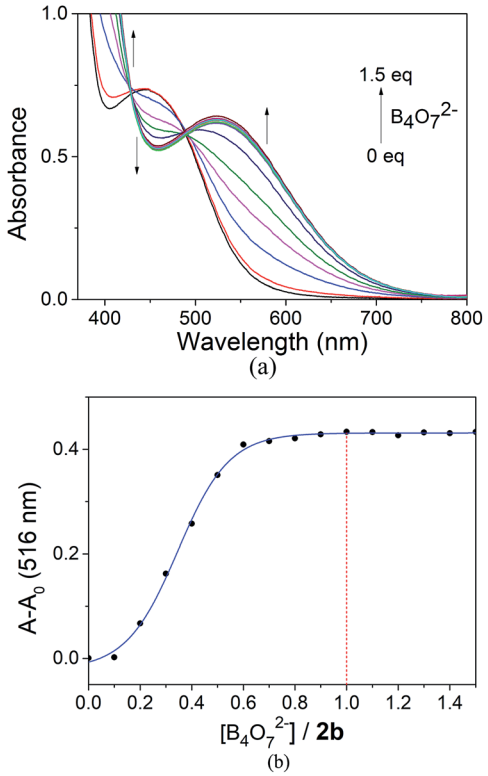

Fig. 7 (a) Absorbance spectra of **2b** with $B_4O_7^{2-}$. (b) Relative absorbance at 516 nm of **2b** in the presence of $B_4O_7^{2-}$ at different $B_4O_7^{2-}$: **2b** ratios.

2.7 Mechanism study

The mechanism of **2b** binding to $B_4O_7^{2-}$ was determined by conducting ^1H NMR titration experiments and theoretical calculations. The chemical shifts of **2b** were calculated based on the optimized geometry. The calculations were performed with the hybrid density functional B3LYP[19,20] and the 6-311++G** basis set using Gaussian 03 [21] (Fig. 10). Hydrogen atoms (H_1–H_7) on the phenanthrene are labeled with chemical shifts. H_1 and H_4 stand for the first and the fourth biggest chemical shift values, correspondingly.

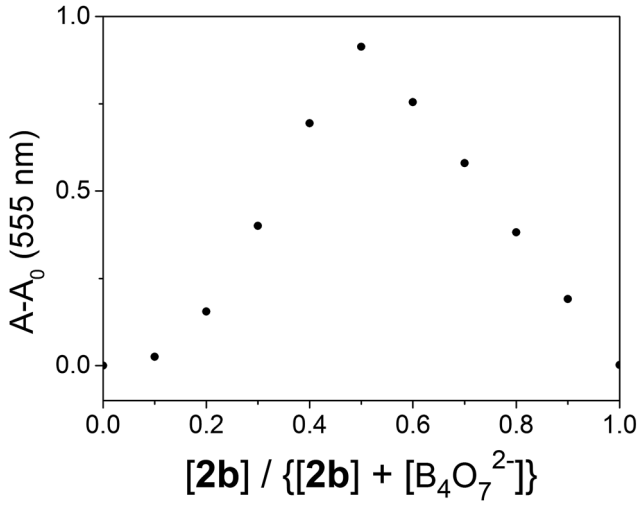

Fig. 8 Job's plot of the interaction of **2b** with $B_4O_7^{2-}$ in DMSO/H_2O (4 : 1).

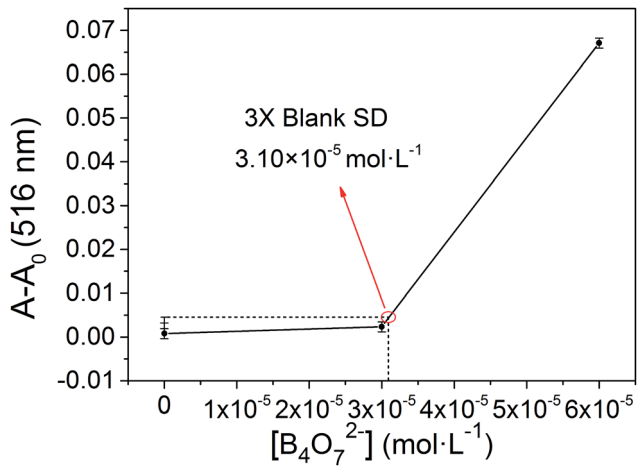

Fig. 9 The absorbance of various $B_4O_7^{2-}$ concentrations measured with respect to the absorbance of the blank.

According to the ^{1}H NMR titration experiments (Fig. 11), the chemical shifts of H_1–H_7 are in the range of 7.4–9.4 ppm. The chemical shifts of most peaks in the NMR spectrum moved upfield as the equiv. of $B_4O_7^{2-}$ increased. Only the peaks of H_1 and H_4 shifted upfield at equiv. less than 0.25 and then downfield in response to further increases in equiv. of $B_4O_7^{2-}$.

Based on the ^{1}H NMR titration and the calculation results, the following mechanism is proposed (Scheme 2). The static force of borate anion toward **2b** and hydrogen bonds between H_1/H_4 and two oxygen atoms of $B_4O_7^{2-}$ are converse interaction. Two boron atoms of $B_4O_7^{2-}$, as an electron-deficient element bind readily with two oxygen atoms of the nitro. This event leads to all peaks in the spectra of **2b** shifting upfield initially. The peaks of H_1 (9.4 ppm) and H_4 (8.6 ppm) shift downfield at higher $B_4O_7^{2-}$ equiv. because of the formation of hydrogen bonds between H_1/H_4 and two oxygen atoms of $B_4O_7^{2-}$, which support the results of the theoretical calculations.

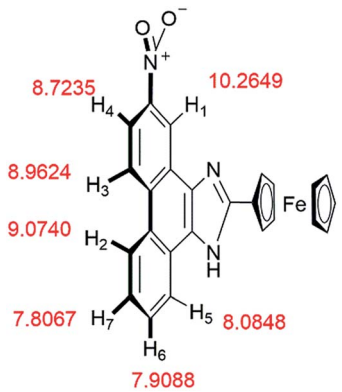

Fig. 10 Chemical shifts of compound **2b** calculated by Gaussian 03.

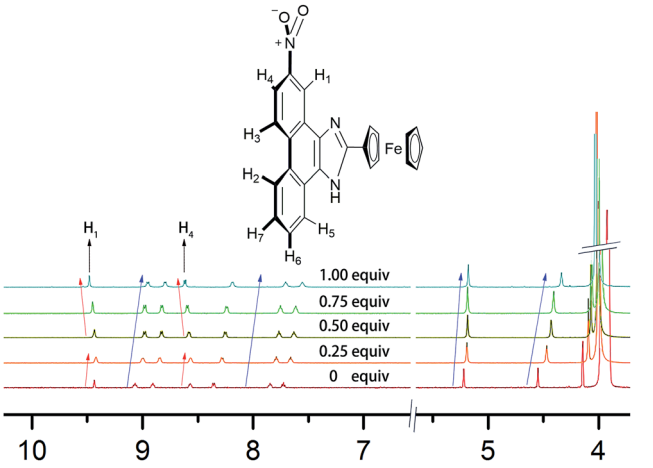

Fig. 11 ^{1}H NMR titration spectra of **2b** in DMSO-d_6 in the presence of various equivalents $B_4O_7^{2-}$ in D_2O.

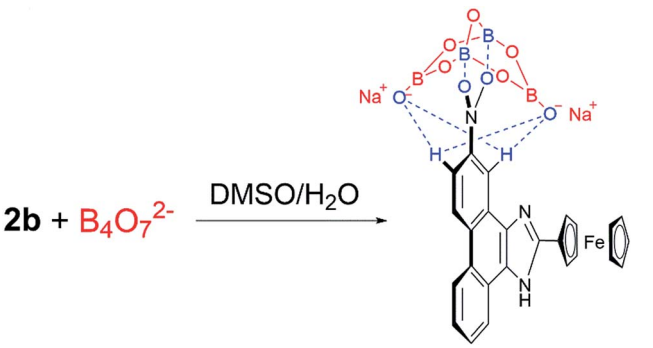

Scheme 2 Proposed mechanism describing how **2b** detects borate ions.

3. Detection of $B_4O_7^{2-}$ in lake water

To evaluate whether our colorimetric probe can detect $B_4O_7^{2-}$ anion in actual samples, we found some samples in the lakes of Yuanming Yuan (the Old Summer Palace) in Beijing. The insoluble substances were removed by filtration. Then **2b** was

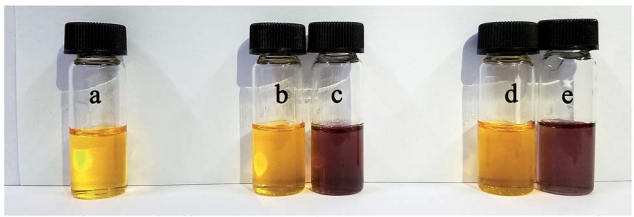

Fig. 12 Influence of different water samples on colorimetric properties of **2b** (a) **2b**; (b) **2b** and sample**1**; (c) **2b**, sample **1** and $B_4O_7^{2-}$; (d) **2b** and sample **2**; (e) **2b**, sample **2** and $B_4O_7^{2-}$. The solvents in bottle a was the mixture of DMSO and deionized water ($V_{DMSO} : V_{H_2O} = 4 : 1$). The solvents in bottle b–e were the mixture of DMSO and lake water ($V_{DMSO} : V_{H_2O} = 4 : 1$).

added in. We observed that sample **1** and **2** showed the same yellow color (Fig. 12(b) and (d)). UV-Vis spectroscopy was used to study the two samples and it showed that no obvious change was found (Fig. 13). It manifested that concentration of $B_4O_7^{2-}$ anion in sample **1** and **2** was below the limit of detection. When $B_4O_7^{2-}$ anion was added into sample **1** and **2**, the color changed from yellow to violet immediately and the change in the spectrum was caused by a bathochromic shift in the absorption maxima from 436 to 516 nm (Fig. 12(c, e) and 13(a, b) the blue curves). It means that the receptor could be used to determine the $B_4O_7^{2-}$ anion in actual samples.

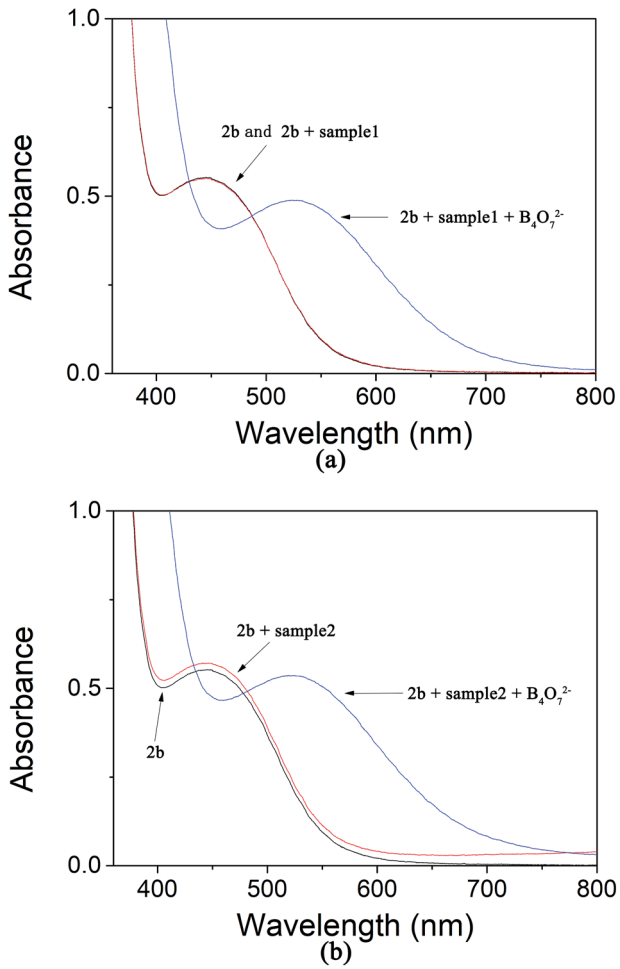

Fig. 13 (a) The absorption of **2b** in the water samples **1**; (b) the absorption of **2b** in the water samples **2**.

4. Conclusions

The syntheses of new ferrocenyl phenanthroimidazole derivatives **2a–2d** have been achieved using simple and short synthetic routines from ferrocene. The introduction of a nitro group to receptor **2a** to afford **2d** gave rise to a prominent color change, and **2b** and **2d** formed 1 : 1 complexes with the borate anion. Both **2b** and **2d** showed good selectivity toward the borate anion when testing the 12 anions, and selectivity was visibly detected by a color change of the reaction solution.

5. Experimental section

5.1 Instruments and reagents

All solvents in the experiments were treated with 5 Å molecular sieves. Melting points were determined using a WRS-1B microscopic and a melting point instrument (Shanghai YiCe Apparatus & Equipment Co. Ltd) without correction. NMR spectra were acquired on a Varian Mercury 600. ^{1}H NMR and ^{13}C NMR were calibrated using tetramethylsilane. Infrared spectra were measured on a Bruker Tensor 27 Infrared spectrometer. Mass spectra were obtained using a Bruker APEXIIFT-ICR mass spectrometer. Crystal diffraction analysis was performed using a AFC10/Saturn 724+ X-ray Single Crystal Diffractometer. Compounds **1a** and **1b** were prepared according to literature.[22,23] Compounds **2a** and **2d** were prepared according to literature.[16,18]

5.2 Synthesis of target compounds 2b–2d

A general method was used to synthesize **2b–2d**, and we provide the method for synthesis of **2b**. In a 100 mL three neck flask, 1-formylferrocene (0.32 g, 1.5 mmol), 2-nitrophenanthraquinone (0.38 g, 1.5 mmol), ammonia acetate (0.58 g, 7.5 mmol) and 20 mL anhydrous methanol were mixed. The temperature was held at ~65 °C and the solution left overnight. The mixture was cooled to room temperature and poured into a 30 mL mixture of ice and water. A brown-red solid was precipitated when the pH value was adjusted to 8. After filtration and washing with dichloromethane, the brown-red product **2b** was obtained.

2-Ferrocenyl-1*H*-2-nitrophenanthro[9,10-*d*]imidazole (2b). 580 mg brown-red solid, yield: 86.8%. Mp >270 °C; ^{1}H NMR (DMSO-d_6, 600 MHz): δ 13.24 (d, J = 85.5 Hz, 1H), 9.38 (dd, J = 135.2, 2.4 Hz, 1H), 9.09 (dd, J = 13.5, 9.2 Hz, 1H), 8.93 (dd, J = 23.7, 8.3 Hz, 1H), 8.57 (dd, J = 16.5, 7.9 Hz, 1H), 8.32 (ddd, J = 8.7, 4.8, 2.5 Hz, 1H), 7.85 (dt, J = 31.0, 7.4 Hz, 1H), 7.75–7.66 (m, 1H), 5.20 (d, J = 29.6 Hz, 2H), 4.58–4.51 (m, 2H), 4.17 (d, J = 2.3 Hz, 5H); ^{13}C NMR (DMSO-d_6, 151 MHz): δ 151.8, 145.7, 145.6, 138.2, 136.6, 131.4, 131.2, 129.0, 128.4, 128.0, 126.9, 126.4, 126.2, 126.0, 125.8, 125.7, 125.6, 125.4, 125.0, 123.5, 122.3, 122.2, 121.9, 118.0, 117.7, 117.3, 109.7, 74.4, 69.8, 69.5,

67.3, 67.2; HRMS (Thermo Q Exactive) calcd for $C_{25}H_{17}FeN_3O_2$ 448.0743, found 448.0730.

2-(1′-Acetyl)ferroenyl-1*H*-phenanthro[9,10-*d*]imidazole (2c). 378 mg, brown solid, yield: 56.5%. Mp >236 °C; ^{1}H NMR (DMSO-d_6, 600 MHz): δ 13.02 (s, 1H), 8.87 (d, J = 8.3 Hz, 1H), 8.83 (d, J = 8.3 Hz, 1H), 8.54 (d, J = 7.9 Hz, 1H), 8.46 (d, J = 7.9 Hz, 1H), 7.78–7.73 (m, 1H), 7.73–7.68 (m, 1H), 7.66–7.59 (m, 2H), 5.25 (s, 1H), 4.75 (s, 1H), 4.56 (s, 1H), 4.52 (s, 1H), 2.11 (s, 3H); ^{13}C NMR (DMSO-d_6, 151 MHz): δ 201.2, 149.0, 137.3, 127.8, 127.6, 127.5, 127.4, 127.3, 125.4, 125.3, 124.5, 124.1, 122.7, 122.4, 122.3, 80.8, 77.5, 73.8, 73.7, 71.4, 71.0, 68.6, 27.7; HRMS (Thermo Q Exactive) calcd for $C_{27}H_{20}FeN_2O$ 445.0998, found 445.0997.

2-(1′-Acetyl)ferrocenyl-1*H*-(2-itrophenanthro)[9,10-*d*]imidazole (2d). 490 mg, brown red solid, yield: 66.7%. Mp >194 °C; ^{1}H NMR (DMSO-d_6, 600 MHz): δ 13.29 (d, J = 84.7 Hz, 1H), 9.37 (d, J = 120.7 Hz, 1H), 9.11 (s, 1H), 8.94 (d, J = 24.3 Hz, 1H), 8.56 (d, J = 23.9 Hz, 1H), 8.34 (s, 1H), 7.86 (d, J = 31.7 Hz, 1H), 7.72 (s, 1H), 5.26 (d, J = 32.7 Hz, 2H), 4.78 (s, 2H), 4.57 (d, J = 34.2 Hz, 4H), 2.10 (d, J = 4.5 Hz, 3H); ^{13}C NMR (DMSO-d_6, 151 MHz): δ 200.8, 150.0, 149.9, 145.7, 145.6, 138.3, 136.5, 131.5, 131.4, 129.1, 128.5, 128.1, 127.1, 126.4, 126.4, 126.3, 126.0, 125.8, 125.7, 125.4, 125.0, 123.5, 122.2, 121.9, 118.2, 117.7, 117.2, 80.5, 76.4, 73.4, 71.3, 70.7, 68.4, 68.4, 27.3; HRMS (Thermo Q Exactive) calcd for $C_{27}H_{19}FeN_3O_3$ 490.0849, found 490.0845.

Conflicts of interest

There are no conflicts to declare.

Acknowledgements

We gratefully acknowledge the financial support by the Beijing Natural Science Foundation (No. 2173060) and the General Plan of Beijing Municipal Education Commission (No. KM201710028007).

Notes and references

1 S. Quintal, M. C. Gimeno, A. Laguna and M. J. Calhorda, *J. Organomet. Chem.*, 2010, **695**, 558.
2 V. O. Nyamori, D. Onyancha, C. W. McCleland, C. Imrie and T. I. A. Gerber, *J. Organomet. Chem.*, 2009, **694**, 1407.
3 S. Quintal, J. Matos, I. Fonseca, V. Félix, M. G. B. Drew, N. Trindade, M. Meireles and M. J. Calhorda, *Inorg. Chim. Acta*, 2008, **361**, 1584.
4 S. S. Yan, L. Q. Jing and Q. Shuai, *Polyhedron*, 2017, **126**, 252.
5 F. Zapata, A. Caballero, A. Espinosa, A. Tárraga and P. Molina, *J. Org. Chem.*, 2009, **74**, 4787.
6 R. Pandey, R. K. Gupta, M. Shahid, B. Maiti, A. Misra and D. S. Pandey, *Inorg. Chem.*, 2012, **51**, 298.
7 J.-L. Thomas, J. Howarth and A. M. Kennedy, *Molecules*, 2002, **7**, 861.
8 J. B. Zhuo, X. Q. Yan, X. X. Wang, L. L. Xie and Y. F. Yuan, *Chin. J. Org. Chem.*, 2015, **35**, 1090.
9 J. B. Zhuo, Q. Wan, X. Q. Yan, L. L. Xie and Y. F. Yuan, *Chem. J. Chin. Univ.*, 2015, **36**, 477.
10 L. L. Ma, T. H. Leng, K. Wang, C. Y. Wang, Y. J. Shen and W. H. Zhu, *Tetrahedron*, 2017, **73**, 1306.
11 S. Saha, A. Ghosh, P. Mahato, S. Mishra, S. K. Mishra, E. Suresh, S. Das and A. Das, *Org. Lett.*, 2010, **12**, 3406.
12 M. Alfonso, A. Espinosa, A. Tárraga and P. Molina, *Org. Lett.*, 2011, **13**, 2078.
13 M. Alfonso, A. Tárraga and P. Molina, *Org. Lett.*, 2011, **13**, 6432.
14 J. C. Wang, Z. M. Chen, L. Qiao, Y. X. Li, X. L. Jiao and Y. R. Jin, *Chin. J. Synth. Chem.*, 2012, **20**, 324.
15 X. F. Wu, P. Wu, J. Y. Li, J. Lu and J. C. Wang, *Chin. J. Org. Chem.*, 2017, **37**, 1412.
16 J. C. Wang, X. F. Wu, X. L. Jiao and M. Wang, *Chin. J. Synth. Chem.*, 2014, **22**, 174.
17 N. Xie, K. Feng, B. Chen, L. Zhang, Z. H. Tong and L. Z. Wu, *Imaging Sci. Photochem.*, 2011, **29**, 45.
18 A. Jaffe, A. S. Valdes and H. I. Karunadasa, *Chem. Mater.*, 2015, **27**, 3568.
19 A. D. Becke, *J. Chem. Phys.*, 1993, **98**, 5648.
20 C. Lee, W. Yang and R. G. Parr, *Phys. Rev. B: Condens. Matter Mater. Phys.*, 1988, **37**, 785.
21 M. J. Frisch, G. W. Trucks, H. B. Schlegel, G. E. Scuseria, M. A. Rob, J. R. Cheeseman, J. A. Montgomery Jr, T. Vreven, K. N. Kudin, J. C. Burant, J. M. Millam, S. S. Iyengar, J. Tomasi, V. Barone, B. Mennucci, M. Cossi, G. Scalmani, N. Rega, G. A. Petersson, H. Nakatsuji, M. Hada, M. Ehara, K. Toyota, R. Fukuda, J. Hasegawa, M. Ishida, T. Nakajima, Y. Honda, O. Kitao, H. Nakai, M. Klene, X. Li, J. E. Knox, H. P. Hratchian, J. B. Cross, V. Bakken, C. Adamo, J. Jaramillo, R. Gomperts, R. E. Stratmann, O. Yazyev, A. J. Austin, R. Cammi, C. Pomelli, J. W. Ochterski, P. Y. Ayala, K. Morokuma, G. A. Voth, P. Salvador, J. J. Dannenberg, V. G. Zakrzewski, S. Dapprich, A. D. Daniels, M. C. Strain, O. Farkas, D. K. Malick, A. D. Rabuck, K. Raghavachari, J. B. Foresman, J. V. Ortiz, Q. Cui, A. G. Baboul, S. Clifford, J. Cioslowski, B. B. Stefanov, G. Liu, A. Liashenko, P. Piskorz, I. Komaromi, R. L. Martin, D. J. Fox, T. Keith, M. A. Al-Laham, C. Y. Peng, A. Nanayakkara, M. Challacombe, P. M. W. Gill, B. Johnson, W. Chen, M. W. Wong, C. Gonzalez and J. A. Pople, *Gaussian 03*, Gaussian Inc., Wallingford, CT, 2003.
22 J. C. P. Mayer, A. C. Sauer, B. A. Iglesias, T. V. Acunha, D. F. Back, O. E. D. Rodrigues and L. Dornelles, *J. Organomet. Chem.*, 2017, **841**, 1.
23 A. Vecchi, N. R. Erickson, J. R. Sabin, B. Floris, V. Conte, M. Venanzi, P. Galloni and V. N. Nemykin, *Chemistry*, 2015, **21**, 269.

